HERMES: revisions in the design for a high-resolution multi-element spectrograph for the AAT

Samuel C. Barden[*a], Damien J. Jones[b], Stuart I. Barnes[c], Jeroen Heijmans[a], Anthony Heng[a], Greg Knight[d], David R. Orr[a], Greg A. Smith[a], Vladimir Churilov[a], Jurek Brzeski[a], Lewis G. Waller[a], Keith Shortridge[a], Anthony J. Horton[a], Don Mayfield[a], Roger Haynes[e], Dionne M. Haynes[e], Denis Whittard[a], Michael Goodwin[a], Scott Smedley[a], Ian Saunders[a], Peter R. Gillingham[a], Ed Penny[a], Tony J. Farrell[a], Minh Vuong[a], Ron Heald[a], Steve Lee[a], Rolf Muller[a], Ken Freeman[f], Joss Bland-Hawthorn[g], Daniel F. Zucker[a], Gayandhi De Silva[a]

[a]Anglo-Australian Observatory, PO Box 296, Epping NSW 1710, Australia;
[b]Prime Optics, 17 Crescent Road, Eumundi, QLD 4562, Australia;
[c]Department of Physics and Astronomy, University of Canterbury, Private Bag 4800, Christchurch 8140, New Zealand;
[d]Sinclair Knight Merz, 100 Christie Street, Sydney NSW 2065, Australia;
[e] innoFSPEC - Astrophysikalisches institut Potsdam
An der Sternwarte 16, 14482 Potsdam, Germany;
[f] Research School of Astronomy & Astrophysics, Mount Stromlo Observatory, Cotter Road, Weston ACT 2611, Australia;
[g]A28 – Physics, The University of Sydney NSW 2006, Australia

ABSTRACT

The AAO is building an optical high resolution multi-object spectrograph for the AAT for Galactic Archaeology. The instrument has undergone significant design revision over that presented at the 2008 Marseilles SPIE meeting. The current design is a 4-channel VPH-grating based spectrograph providing a nominal spectral resolving power of 28,000 and a high-resolution mode of 45,000 with the use of a slit mask. The total spectral coverage is about 1000 Angstroms for up to 392 simultaneous targets within the 2 degree field of view. Major challenges in the design include the mechanical stability, grating and dichroic efficiencies, and fibre slit relay implementation. An overview of the current design and discussion of these challenges is presented.

Keywords: spectrograph, high resolution, volume phase holographic grating, multi-object, AAT, galactic archeology, fiber

1. INTRODUCTION

A new facility class instrument for the Anglo-Australian Telescope (AAT) is currently in development at the Anglo-Australian Observatory (AAO). This instrument, High Efficiency and Resolution Multi-Element Spectrograph (HERMES), is an optical high-resolution multi-object spectrograph designed primarily for a major survey of ~1 million stars in the Milky Way Galaxy to perform "Galactic Archaeology" to unravel the formation history of the Galaxy. The instrument, to be fed with the existing 2dF robotic fibre positioning system, has undergone significant design revision over that presented at the 2008 Marseilles SPIE meeting[1]. The current design is a 4-channel VPH-grating based spectrograph providing a spectral resolving power of 28,000 standard and a high resolution mode ranging between 40,000 to 50,000 with a slit mask. The total spectral coverage is about 1000 Angstroms for up to 392 simultaneous targets within the 2 degree field of view. The collimator is an f/6.32 off-axis Houghton derivative delivering a 190 mm diameter pupil on the gratings. The entrance slit is a curved array of the fibres that compensates for high order dispersion terms to straighten out the slit curvature on the detector. The output of the fibres are relayed from f/3.15 to

* scb@aao.gov.au; phone +61 2 9372 4852; fax +61 2 9372 4880; aao.gov.au

Ground-based and Airborne Instrumentation for Astronomy III, edited by Ian S. McLean, Suzanne K. Ramsay, Hideki Takami, Proc. of SPIE Vol. 7735, 773509 · © 2010
SPIE · CCC code: 0277-786X/10/$18 · doi: 10.1117/12.856103

f/6.32 with micro-optic relays. Dichroic beam splitters are used to split the light into the four channels. Each channel utilizes fold mirrors, exchangeable VPH gratings, all transmissive camera optics, and a 4k by 4k E2V detector system optimized for the wavelength band of each channel. All surfaces are either spherical or plano except for the first surface of each camera, which is paraboloid. Major challenges in the design include the mechanical stability, grating and dichroic efficiencies, and fibre slit relay implementation. An overview of the current design and discussion of these challenges is presented.

2. SCIENCE OBJECTIVES

HERMES provides an extraordinary and unprecedented opportunity to undertake a million-star archaeological survey of the Galactic stellar disk. This multi-year Galactic Archaeology (GA) observational program will obtain detailed elemental abundances and precise radial velocities for each targeted star. Elemental abundances representing the main nucleogenesis processes in both dwarf and giant stars will allow chemical tagging of the individual stars to their original formation event, and accurate velocities will permit differentiation of stars by their dynamics [2,3,4]. The resulting data sets will yield a comprehensive view of the formation and evolution of the Galactic disk, enabling the reconstruction of the original stellar building blocks of the Galactic disk and address the following basic questions:

- What were the conditions of star formation during early stages of Galaxy assembly?
- When, where and what drove the major episodes of star formation is the disk?
- To what extent is the Galactic disk composed of stars from merger events?
- Under what conditions, and in what types of systems did the accreted stars form?
- How have the stars that formed *in situ* in the Disk evolved dynamically since their birth?
- Where are the solar siblings that formed together with our Sun?

HERMES will also present a tremendous opportunity for scientific synergies with the European Space Agency's GAIA mission. GAIA, a €500 million astrometric satellite scheduled for launch by 2012, will measure precise distances and tangential motions for the majority of HERMES GA survey stars. Precise distances from GAIA will yield accurate ages for a significant fraction of those stars, which will allow direct determination of the evolution of elemental abundances with time in the disk of the Milky Way, as well as providing critical information for studies of stellar astrophysics Transverse velocities, in conjunction with the radial velocities measured by HERMES, will give a complete picture of the space motion for each star, and hence identify spatially-mixed stars with a common origin through their similar dynamics. The combination of HERMES abundances and radial velocities along with GAIA astrometry will provide a truly extraordinary legacy for unravelling the history of the Milky Way Galaxy.

In addition to the GA objectives, HERMES will be a powerful instrument for the study of stellar astrophysics, the interstellar medium, and the Magellanic Clouds. Table 1 provides a summary of the observational requirements for each of the different science cases envisioned for the HERMES instrument.

Table 1. Summary of observational requirements for HERMES science.

Requirement	**Galactic Archaeology**	**Stellar Astrophysics**	**Interstellar Medium**	**Radial Velocity Variability**
Brightness of Targets (V mag)	10–14 for main GA survey; down to 16 – 17 for targeted observations	Typically brighter than 14	Wide range; not strictly relevant for emission-line objects	Typically brighter than 14
Wavelength Windows (Å)	4708Å – 4893Å 5649Å – 5873Å 6481Å – 6739Å 7590A – 7890Å	Wide range; in some cases GA wavelength windows appropriate	Wide range across optical spectrum	Wide range; if using iodine cell, 4800Å – 6000Å
Spectral Resolution ($\lambda/\Delta\lambda$)	~30,000	~30,000; ~50,000	~30,000; ~50,000	~50,000
Sensitivity (SNR)	100 at V~14 in 1 hour (GA survey)	Wide range	Wide range	Wide range

3. HERMES DESIGN

1. Optical Design

The initial concept for HERMES was based upon a white pupil echelle configuration that made use of the existing AAOmega hardware[1]. The design was significantly altered when it was decided to make HERMES a separate standalone instrument in order to minimize the downtime impact on AAOmega. A subsequent cost tradeoff study revealed that a multi-channel instrument utilizing first order volume-phase holographic (VPH) gratings was preferable over the white pupil echelle design. A four-channel instrument design was developed providing nearly 1000 Å of total spectral coverage for optimal wavelength coverage for the GA survey and flexible reconfiguration (by exchanging gratings) required for the alternative scientific objectives. Fig 1 shows the optical design and the coordinate reference frame.

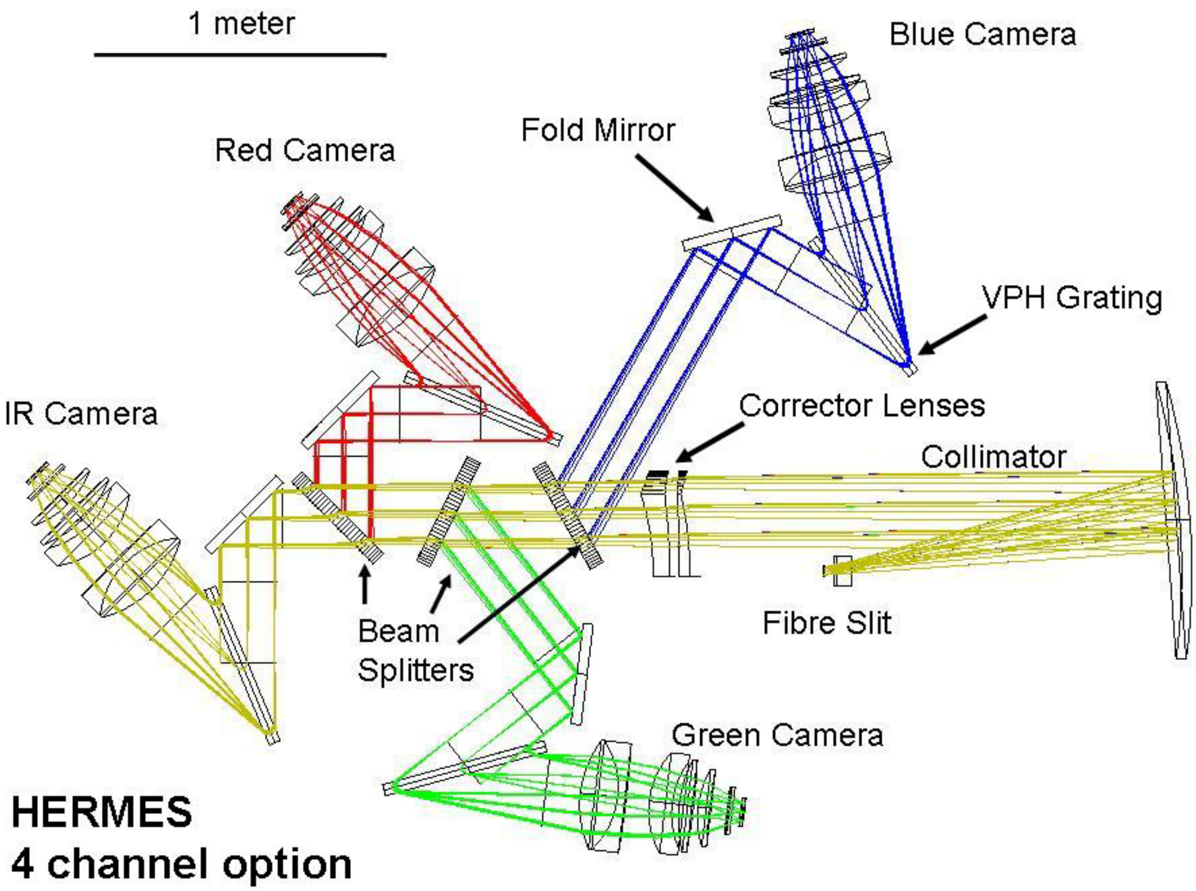

Fig 1. Optical schematic of the HERMES spectrograph looking down with spectral dispersion in the plane of the figure. The bottom figure shows the global reference frame with the x-axis pointing into the plane of the figure.

The primary design characteristics are:

- 2 degree field of view (2dF facility)
- Two 392 fibre slits (one for each 2dF field plate)
- Fixed configuration (no camera articulation or grating rotation)
- Curved slit to compensate for wavelength curvature from the grating
- Off-axis f/6.3 collimator, modified Houghton design

- 190 mm beam diameter
- R2.5 (68°) VPH gratings
- Exchangeable gratings and beam splitters
- 4 channels
- 3 dichroic beam splitters
- f/1.7 cameras
- All spherical optics except for front surface of each camera
- Front surface of each camera is a paraboloidal surface
- Red and IR cameras are identical
- 4k by 4k pixel detectors (E2V)
- 15 micron pixels
- ~4 pixel sampling at R~28,000
- Optional slit mask for R~45,000

The wavelength bands for the GA science and the usable wavelength bands for each channel are shown in Fig 2. Changing wavelengths from the GA bands requires a different grating, possibly a different beam splitter, and a refocus of the cameras (piston and tilt).

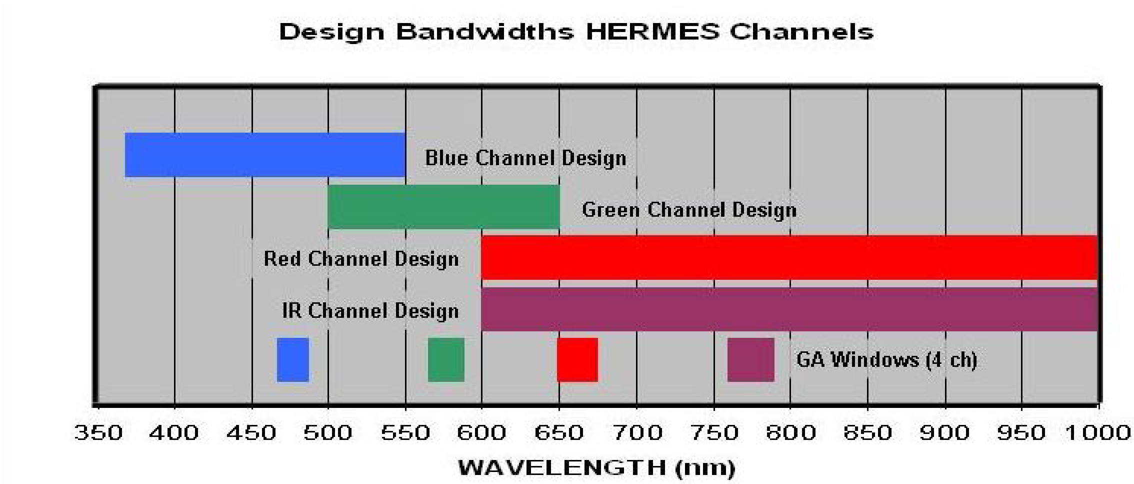

Fig 2. Wavelength bands for the HERMES channels and GA spectral windows.

Details on the following components of HERMES will be discussed in the remainder of this paper.

- Fibre cable and slit assembly
- Beam splitters
- VPH gratings
- Cameras and detectors
- Space frame and spectrograph lab
- Grating ghosts
- Efficiency model
- Control system
- Calibration
- Data reduction and abundance analysis

2. Fibre cable and slit assembly

The 2dF facility has two field plates. While one is in the observing position the other is aligned with the robotic positioner for reconfiguration for the next target field. A tumbler swaps the two plates in between target field observations. 400 fibre positions are available around the circumference of each of the two 2dF field plates. Eight of these positions are utilized by fibre guide probes that feed to a guide TV. The remaining 392 positions are for science targets and sky observations. The science fibres will run a length of about 40 metres to the HERMES spectrograph in 40 groups of 10 fibres for each field plate. The fibres have a 140µm core diameter and a 198µm outer diameter including the cladding and buffer. Each science fibre probe in 2dF will contain two fibres: one for AAOmega and one for HERMES. The robotic positioner software will configure the probe according to which instrument is in use. The full fibre cable will house a minimum of 1568 fibres (two sets of 392 fibres to both AAOmega and HERMES) plus spares. Consideration is underway to add back the eight missing fibres from each field plate with fibres that are linked to a calibration source for simultaneous wavelength calibration.

Exploration was made for implementing a fibre connector rather than having two fibres in the 2dF science probes. The dual fibre probe approach was selected after cost and feasibility comparisons with the connector showed the dual approach to be less risky and more cost beneficial.

In HERMES, the slit must be curved in order for the detector to see the same wavelength coverage for all fibre apertures. This is due to second order terms in the dispersion from the grating due to out of plane illumination. Fig 3 shows the geometrical arrangement for the fibre slit. The axis of the fibres are aligned such that the pupils all overlap at the grating.

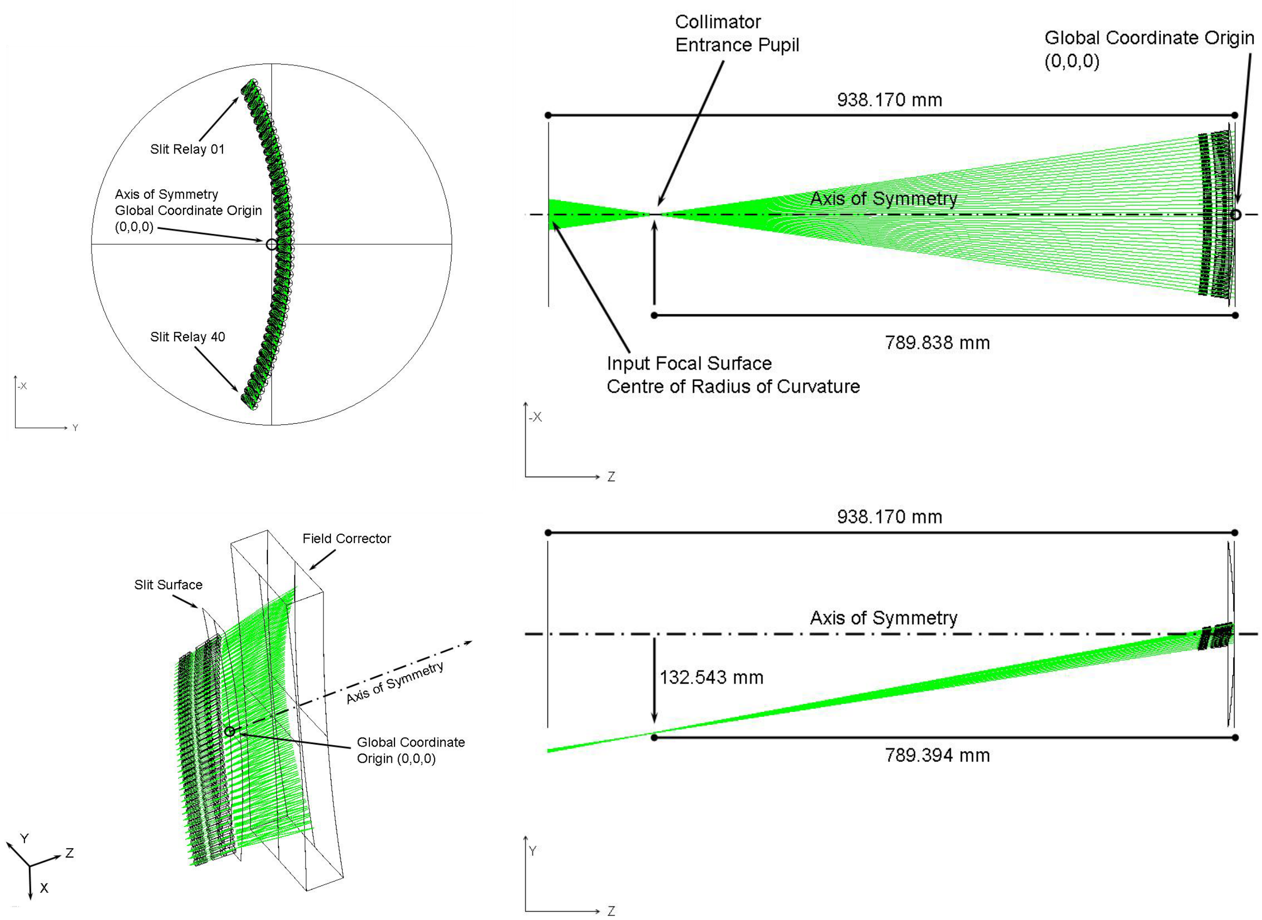

Fig 3. Geometrical configuration of the fibre slit. Upper left is view looking at slit end from collimator along axis of symmetry. Upper right is side view. Lower right is top view.

A lens relay is required in the slit to relay the f/3.15 output of the fibres to the f/6.3 focal ratio of the collimator. This relay allows the collimator to be off-axis so that mechanical components of the curved slit unit do not interfere with the light path. Fig 4 displays the optical schematic of the relay optics and the mechanical concept for the slit unit.

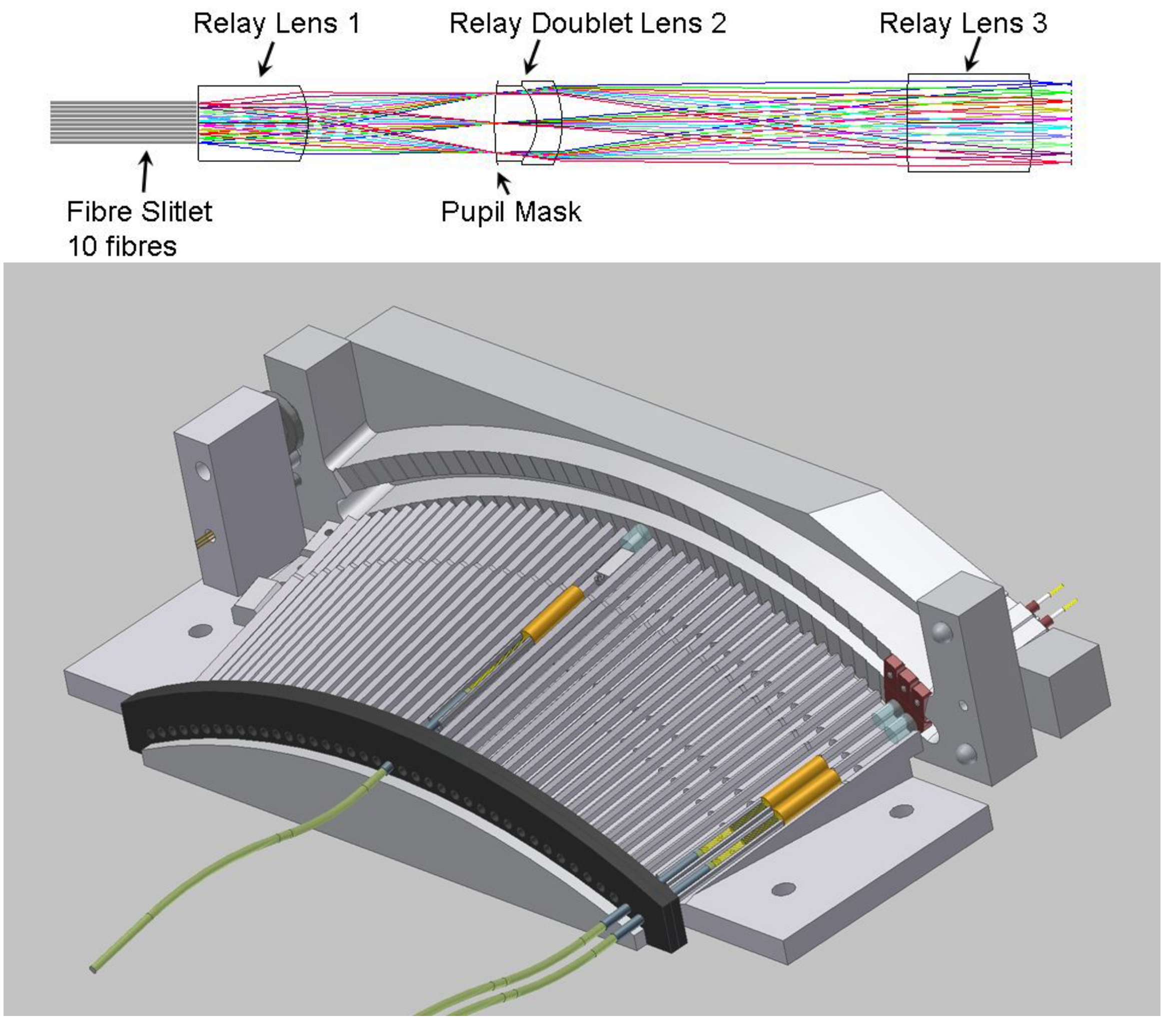

Fig 4. Top figure shows the optical relay. The bottom shows the mechanical concept for the assembly of the slit and relay optics.

When the field plate is reconfigured, the fibres must be back-illuminated so that the robotic positioner can measure the fibre positions. Back illumination ports are required to provide such illumination. Fig 5 shows the way in which the slits will be alternated between the observing position and the back illumination ports.

For the higher resolution mode, a custom slit mask will be fabricated for both slit assemblies and mounted at the slit image formed by the relay optics. Fig 6 shows the dimensions and orientation of the slit apertures on the mask.

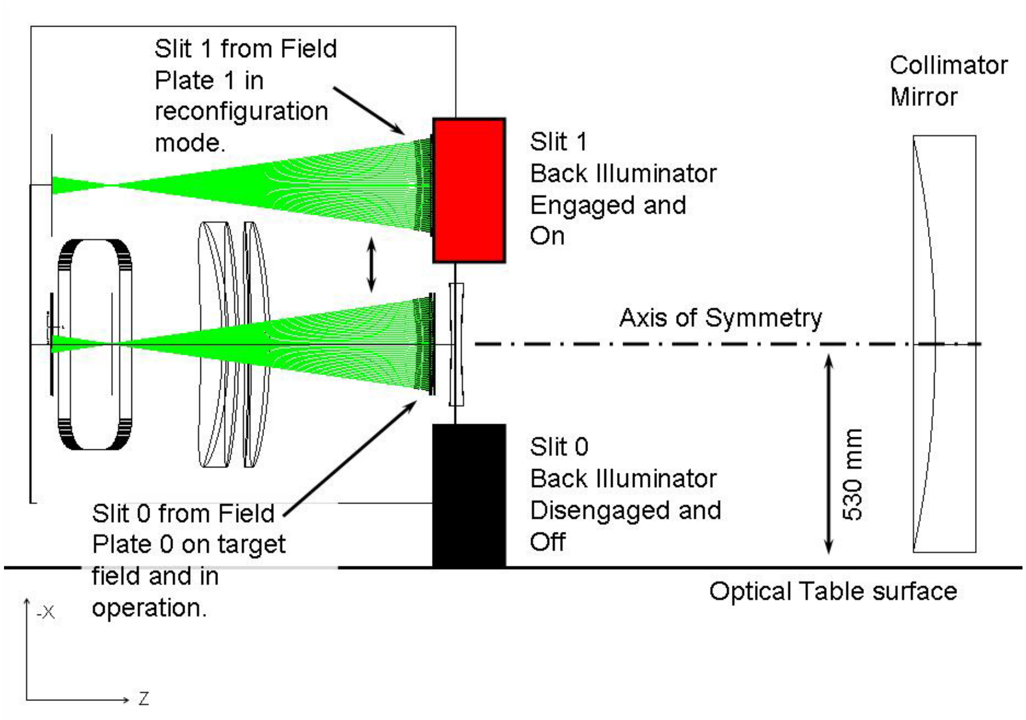

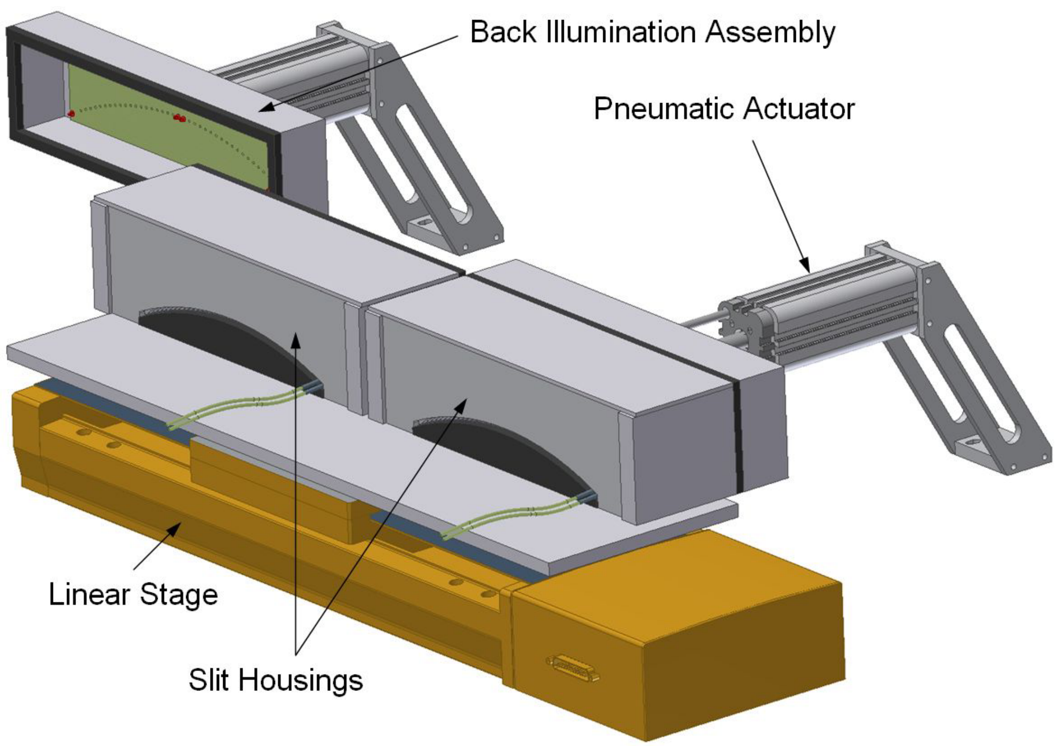

Fig 5. Schematic of the two positions for the HERMES slits. The bottom shows the translation mechanism to move the slits between the back illumination systems.

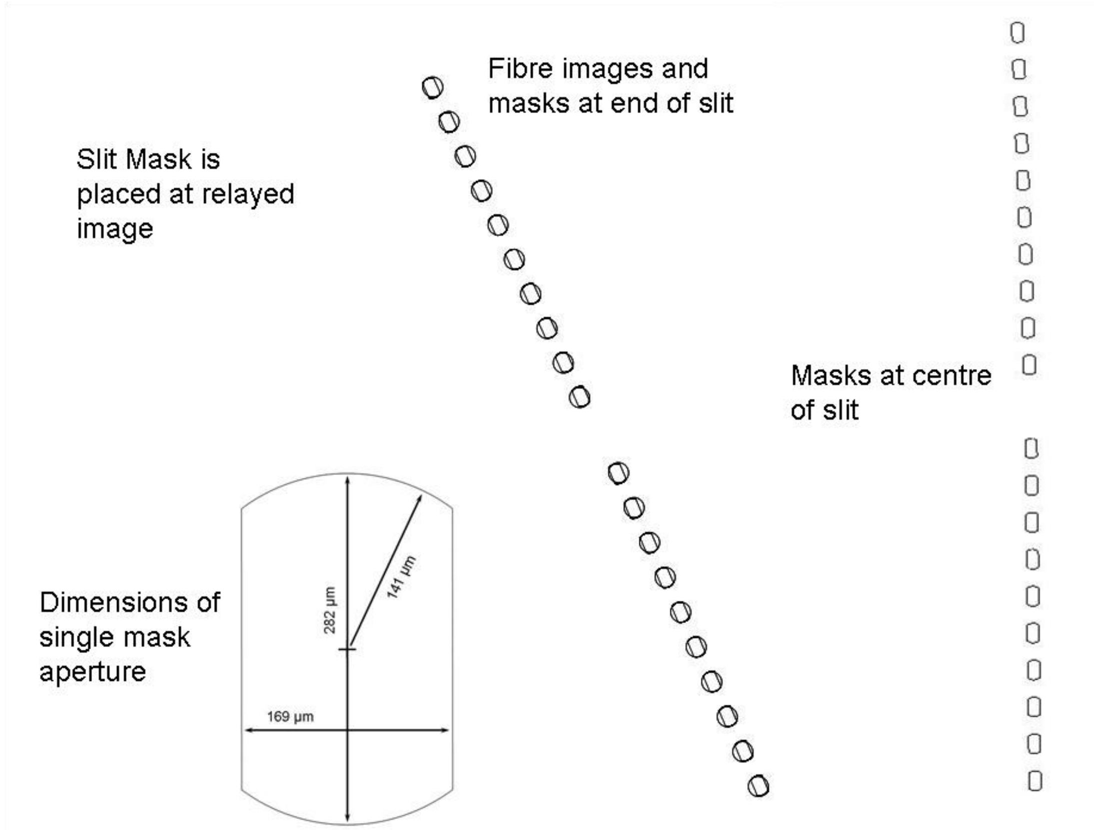

Fig 6. Slit mask apertures for 20 of the 400 fibres.

The analyses on the resulting image quality with the slit mask are shown in Fig 7 for wavelengths ranging 581-587nm. The complete optical model is taken into account. The pixelated resolution for these fibres is calculated to be 52-54,000. β and μ are parameters to match the full width at half maximum (FWHM) and mean of a Gaussian profile fit.

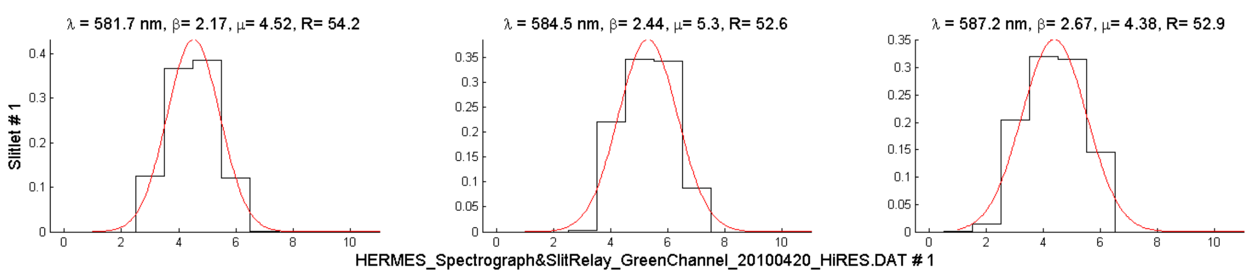

Fig 7. Fibre spectral image profile width on the detector (β in pixels); pixelated fibre image profile (black line), Gaussian profile fit to fibre image profile to calculate resolution, $R\times10^3$,(red line).

3. Beam splitters

The design for the Blue and Green channel beam splitters is not particularly challenging except for the size of the elements required. The footprint of light on the Blue beam splitter is 280 by 530 mm. It was decided to make all beam splitters the same size so to minimize design effort. The illumination angles for the Blue and Green beam splitters are 30°. The illumination angle for the Red beam splitter must be 45° in order to fit in the Red channel. The high angle on the Red beam splitter increases the complexity of the dichroic design for performance in unpolarized light. Fig 8 shows the sizing of the beam splitters and the footprint of light as it progresses through the chain into the IR channel. Fig 9 displays the polarization issue with the Red beam splitter. Fortunately, the GA requirements provide a wide gap between the Red and IR channels. Shifting the wavelength transition blueward would provide adequate unpolarized performance for the GA case.

The requirement that HERMES have four channels of spectral coverage in order to meet the wavelength demands of the GA survey imposes a tight geometrical constraint on the Blue and Red channels (see Fig 1). The grating of the Red channel comes very close to the beam propogating off the Blue beam splitter. The 45°on the Red beam splitter is required to keep the Red channel from obstruction the Blue channel light With a straight slit, there would have been two geometrical solutions for each channel, however, the presence of the curved slit eliminates that symmetry resulting in a constrained geometrical layout.

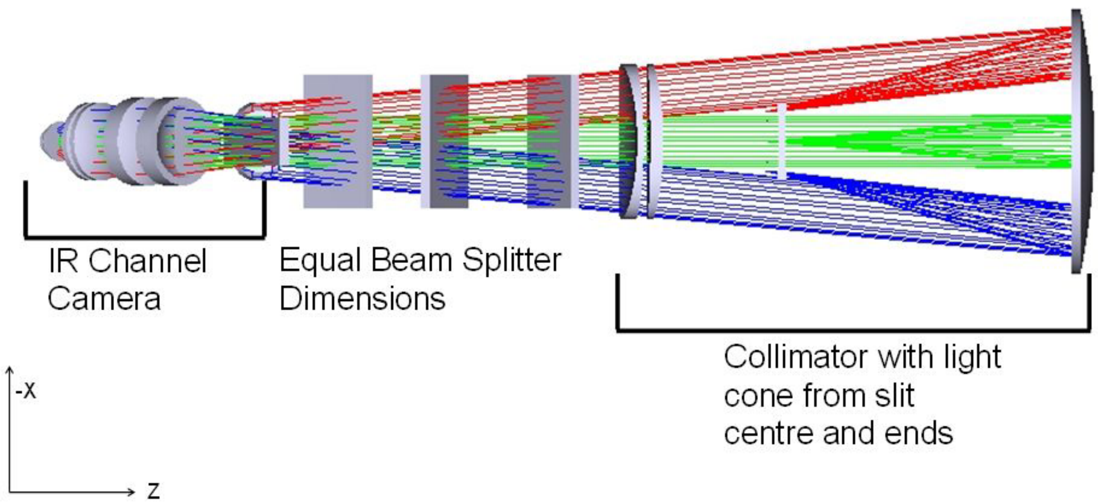

Fig 8. Side view of light path through beam splitters. The pupil from all fibres overlap on the grating.

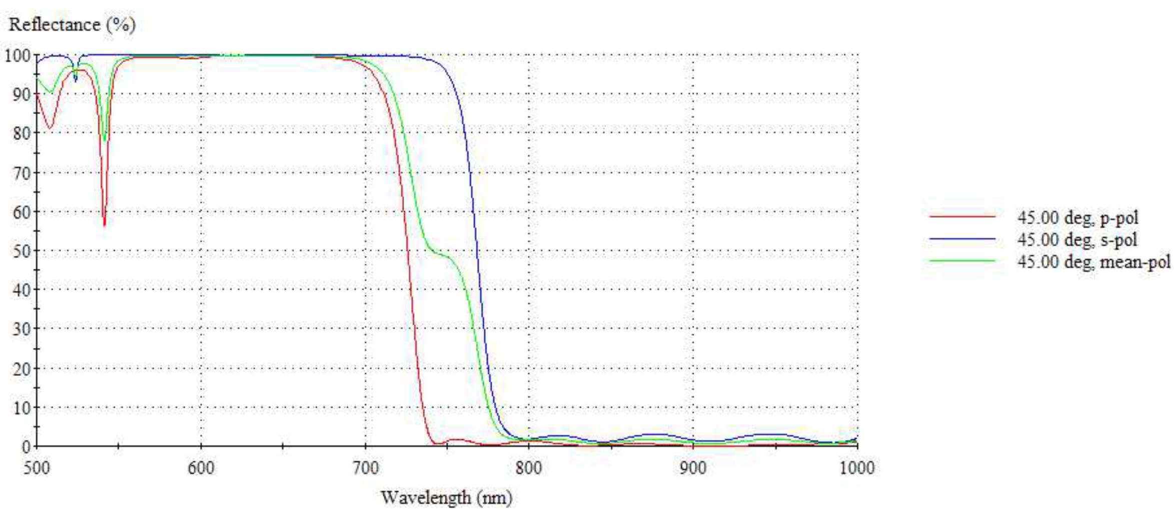

Fig 9. Polarization issue with Red beam splitter at the use angle of 45°. The p-polarization transitions at a significantly bluer wavelength than the s-polarization. (Plot provided by D. Baker, Optical Coatings Associates Pty Ltd, Queensland, Australia)

4. VPH gratings

Volume phase holographic (VPH) gratings will be used to disperse the light. The gratings will be operated in the Littrow condition. In order to match the spectral coverage to the detectors while achieving adequate dispersion with the large aperture fibres and a 190 mm beam, the gratings must operate at a Bragg angle of 67.2°. The axes of the cameras are set to 68.1° to the grating in order to achieve an appropriate balance of the resultant efficiency profile. Table 2 lists the design parameters for the VPH grating set. Fig 10 shows the geometrical illumination for the gratings.

Table 2. Parameters for HERMES GA survey gratings.

Grating	Line Frequency *(l/mm)*	Bragg Angle *(deg)*	Bragg Wavelength *(nm)*	Camera Angle *(deg)*	Central Wavelength on detector *(nm)*	Wavelength Band *(nm)*	Band Width *(nm)*
Blue	3835.0	67.2	480.8	68.1	479.0	470.8-489.3	18.5
Green	3196.0	67.2	576.9	68.1	577.4	564.9-587.3	22.4
Red	2785.0	67.2	662.0	68.1	662.6	648.1-673.9	25.8
IR	2379.0	67.2	775.0	68.1	776.0	759.0-789.0	30.0

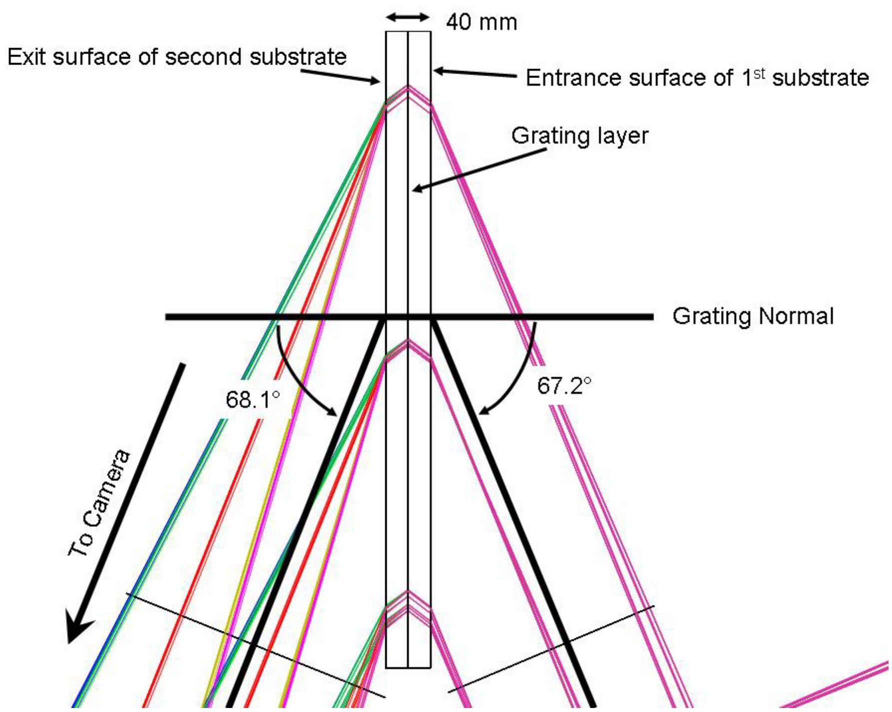

Fig 10. Illumination geometry for the HERMES gratings.

The footprint of light on a grating covers a quasi-ellipse with a major axis of 500 mm and a minor axis of 210 mm. The substrates need to be 240 by 570 mm. This large aperture requires that some of the gratings be made with stitched or mosaiced exposures due to size limitations with all of the vendors capable of producing these gratings.

The high Bragg angle of the VPH grating introduces a significant polarization effect on the achievable bandwidth. Fig 11 shows an efficiency model for the Green grating for a given dn index modulation of 0.06. If the grating is optimized for s-polarization (parallel to the fringe structure) only, a broad bandwidth can be achieved albeit at an efficiency of only 50% of the total light. However, if the grating is pushed to provide good p-polarization as well, the bandwidth is significantly reduced. This reduced bandwidth peaks at a much higher efficiency, but drops below that achieved with the s-polarized efficient grating at the ends of the detector coverage and has higher variability as a function of slit position with variations of a factor of two near the ends of the detector between spectra located near the center and edges of the slit.

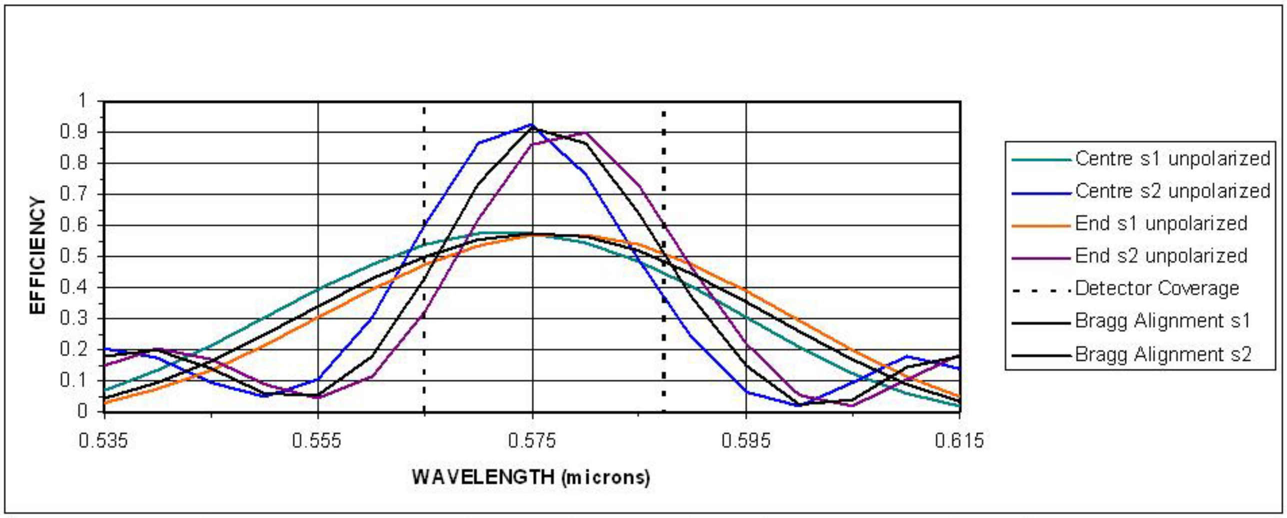

Grating Name	Central Wavelength (nm)	Bragg Wavelength (nm)	Blue Detector Limit (nm)	Red Detector Limit (nm)	l/mm	Bragg Angle (air) (degrees)	dn	d for 1st s peak (microns)	d for 2nd s peak (microns)
HERMES_Green-1	577.4	576.9	564.9	587.3	3196	67.2	0.06	4.0	11.7

Fig 11. Efficiency model for the HERMES Green grating. The three centrally peaked lines are the efficiency achievable with a design optimized for unpolarized light. The leftmost curve is for spectra near the center of the slit, the rightmost curve for spectra near the edge of the slit. The broader lower efficiency curves are for a grating optimized for s-polarization. Again, the leftmost curve is at the center of the slit and the rightmost near the end.

If the *dn* value can be pushed to higher values, the grating thickness can decrease and yield a wider bandwidth. Explorations are underway with the grating vendors to see if adequate bandwidth can be achieved for the unpolarized case without introduction of scattering which is often a consequence of pushing *dn* values to larger values. Fig 12 shows an image of a prototype grating produced by Wasatch Photonics for evaluation.

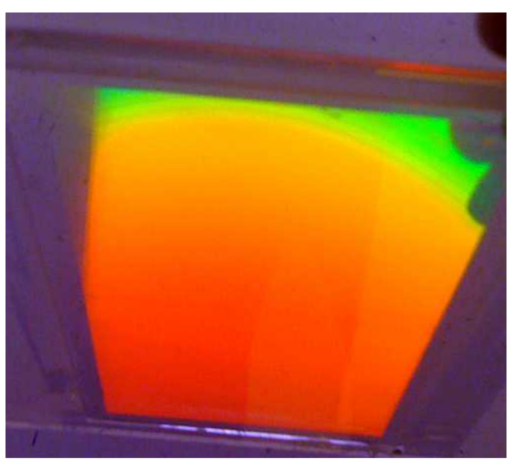

Fig 12. Photo of prototype grating (Wasatch Photonics).

The antireflective (AR) coatings required for the grating substrates is another area of considerable concern. Again, polarization can become an issue with AR coatings having high loss when trying to get both polarization states into and out of the glass. AR coatings may only be ~80% efficient on an unpolarized grating. However, if the grating is optimized for only s-polarization, then the AR coating can be optimized for optimal coupling of the s-polarization state.

If the gratings are also optimized only for the s-polarization state, the issue with the polarization performance of the Red beam splitter also disappears.

The optical configuration for HERMES is independent of the polarization issue. In a worse case scenario, an initial set of gratings that may not be as optimal as desired can eventually be replaced with higher performance gratings if and when the technology allows for their fabrication.

5. Cameras and detectors

The optical layout for a representative camera is shown in Fig 13 and Fig 14.

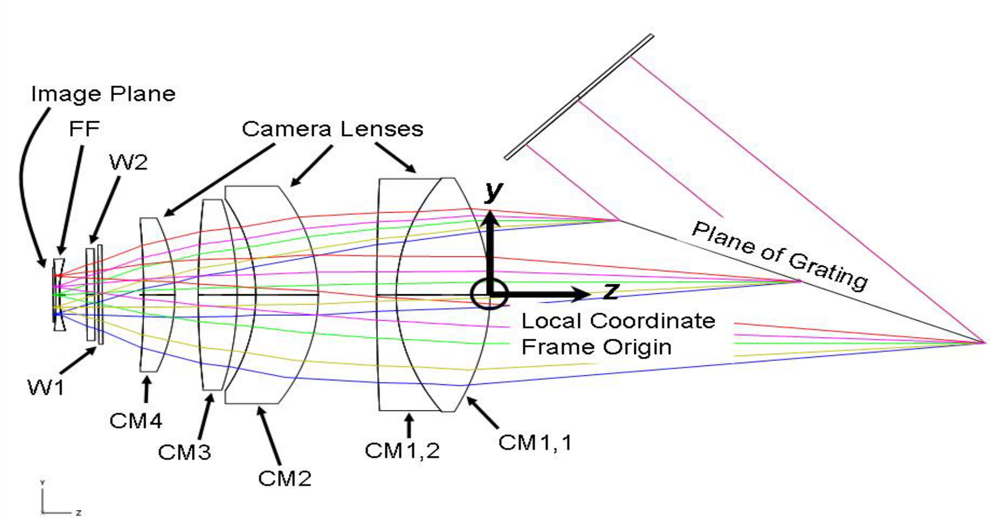

Fig 13. Camera view from above showing 5 wavelengths imaged onto the detector.

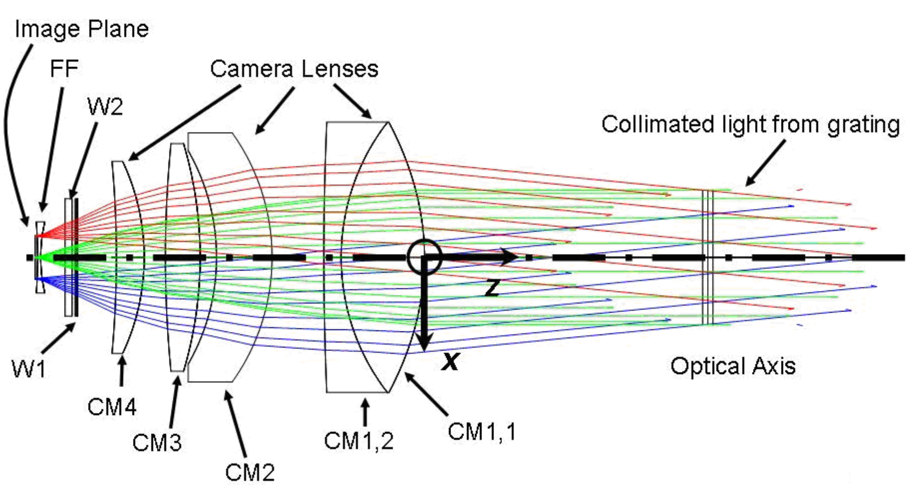

Fig 14. Camera view from side showing three slit positions imaged onto the detector, spectral dispersion is in y-plane.

The Camera Windows W1 and W2, serve three functions: allow light to enter into an evacuated cryostat; provide a dry air environment to prevent dewing or frosting of the windows; and to provide second order blocking for the Red and IR cameras with OG530 glass for element W1. The Camera Field Flattener Lens (FF) produces a flat image plane so that the light can be imaged onto a CCD. Camera focus is achieved by piston and tilt movement of the cryostat assembly containing the Windows, Field Flattener Lens, and CCD.

The detectors used in HERMES are all E2V devices with 4k by 4k pixel formats. Table 3 lists the four detectors being utilized. The IR detector has not yet been purchased as it may be desirable to acquire a deep depletion device that E2V are currently developing. Fig 15 shows an image of a sample detector. The Blue, Green and Red detectors have already been procured.

Table 3. CCD type for each of the HERMES channels.

Channel	**Device**	**Coating**
Blue	E2V CCD231-84-0-141	Standard 16 micron Astro Broadband
Green	E2V CCD231-84-0-E56	Standard 16 micron Astro Midband
Red	E2V CCD231-84-0-E24	Deep depletion 40 micron Asro ER1 With fringe suppression
IR	E2V CCD231-84-0-E24	TBD

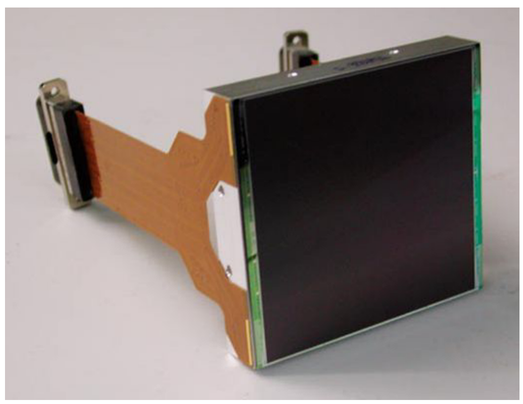

Fig 15. Front View of e2v CCD231-84 Detector (lying on its side)

The detectors will be mounted in a cryostat that insulates the CCD in a vacuum environment. The cryostat will utilize a closed cycle gas cooler to cool the detectors down to 113 Kelvin. The cryo-cooler has a heat exchanger outside the spectrograph room and a cold head which is mounted in the cryostat. One cryostat has currently been built to characterize the detectors and controllers. Fig 16 displays a schematic of the cryostat design which is made from an IR-Lab cryostat with a custom top hat box for the detector and window optics.

6. Space frame and spectrograph lab

The space frame is designed to achieve a light weight and stiff structure that is dimensionally stable for HERMES. The plate structure is built around the optical components in such a way that the neutral axis falls together with the optical axis. Bending effects of the frame on the optical components will therefore be minimized. The optical components and assemblies weight over a hundred kilograms and require a stiff mount to create a sufficiently high Eigen frequency. The instrument is isolated from the ground vibrations by pneumatic isolators.

Dynamical analyses of the instrument show the Eigen frequencies can be well decoupled from those of the isolators. The isolators are specified to filter out 98% of the floor vibrations above 10 Hz. The Eigen frequency ranges from 3-5Hz where the frame has a rigid body mode on the stiffness of the isolator.

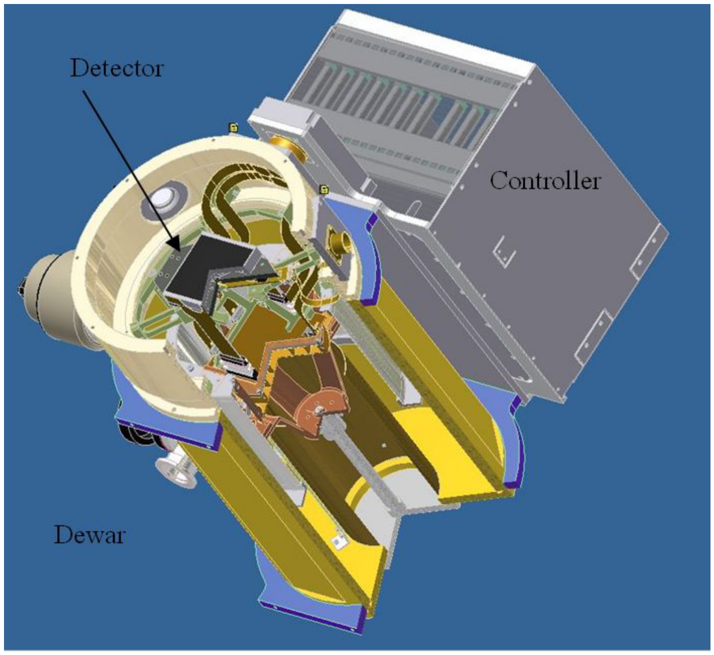

Fig 16. Design of cryostat with cut out and controller box on top.

Thermal stability is achieved by placing the heat sources away from the instrument and by providing insulation and active thermal control of the room. The material choice for the frame is aluminum. The good conductivity (k≈171W/m/K) minimizes the temperature gradients over the 4.5 x 3.5 meter instrument. Temperature gradients result in misalignment of the optical components while homogeneous temperature changes only causes defocusing which is less stringent. The large heat capacity of aluminum (C ≈ 960J/kg/K) means a 0.1 Kelvin temperature variation requires 76.8 kilojoules for a 800 kg structure. This is equivalent to an absorbed power of 21 Watts over one hour. This gives a guide line for the effort needed to control the temperature and dissipated heat.

The required stability can be split up in a long term and a short term stability requirement. The long term stability requirement is set by the required image quality and is determined by the misalignment of the optical components. The short term stability requirement is much more stringent as it is set by the required resolution and accuracy of the spectral measurements. Optical analyses over the full instrument have been performed with realistic assumptions for the individual displacements as thermal drift is interrelated. For the collimator mirror this results in the following values, see Table 4.

A new spectrograph room is being built in the west Coude area of the AA-Telescope to accommodate HERMES. The room is temperature controlled and the heat exchangers are placed outside this area. A new fibre cable runs from the telescope to the instrument with a total estimated length of 45 meters. A bridge crane placed over the instrument gives access to the gratings and beam splitters when they need to be exchanged. Fig 17 shows a solid model for the space frame configuration. The location of HERMES and the spectrograph lab is shown in Fig 18.

Table 4. Stability requirements for the collimator mirror.

Stability	Radial	Axial	Tip/tilt
Long term	200µm	200 µm	30 Arcsec
Short term	<6 µm	<25 µm	<0.5 Arcsec

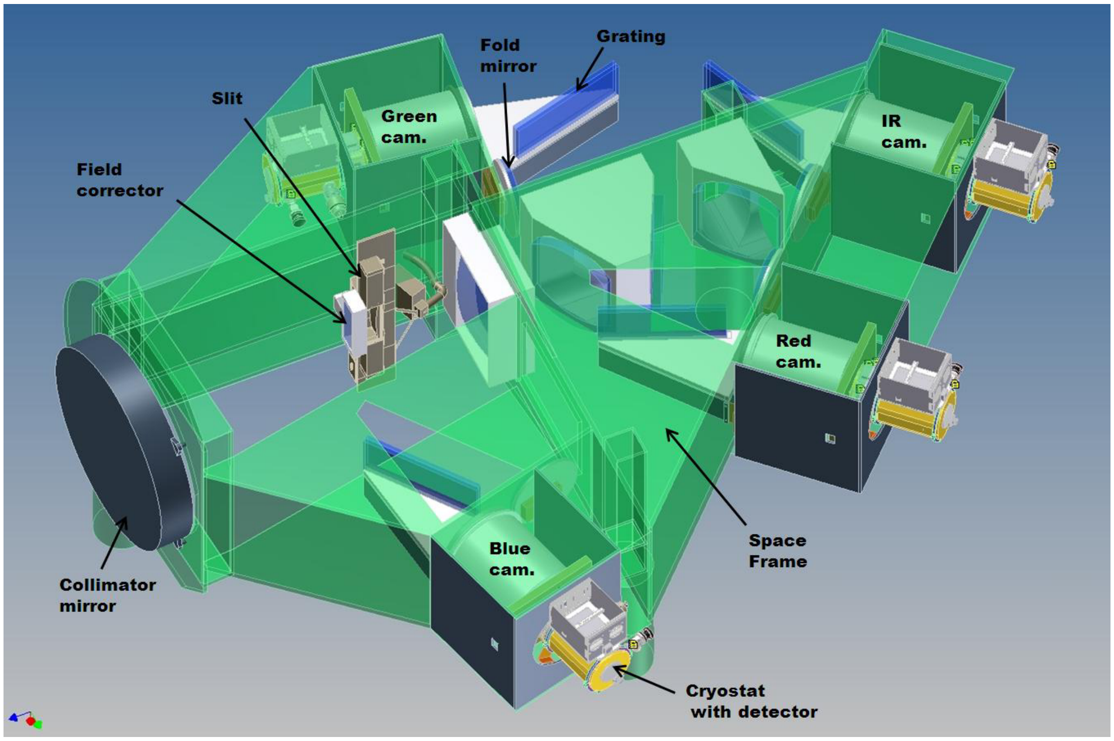

Fig 17. CAD model representation of the HERMES space frame.

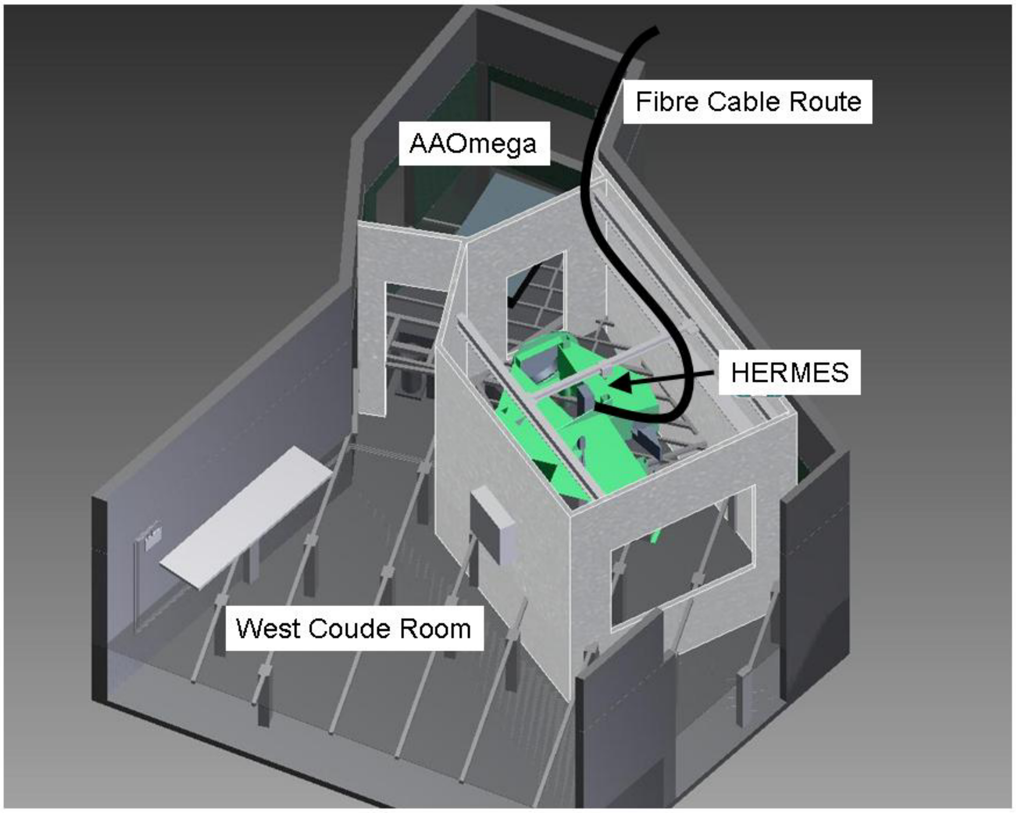

Fig 18. Location of HERMES (green) with respect to spectrograph AAOmega in the West Coude room, AA-Telescope.

7. Grating ghosts

A VPH grating used in a Littrow configuration produces an optical ghost[5]. The ghost is essentially an image of the entrance slit (in this case a fibre aperture) but has components that are in and out of focus. A ghost will be created for each spectrum. The ghost is not spectrally dispersed, as it is a recombined white light image of the slit produced by the grating with light that has been reflected back up to the grating by the detector. This ghost has been seen in the AAOmega spectrograph[6] . The peak amplitude of the ghost on AAOmega is between 0.5 and 1.0% of the continuum of the spectrum producing the ghost. In HERMES, we need to have less than 1% contamination of any spectrum by residual scattered light or cross talk from neighbouring spectra in order to retain the S/N 100 target for the faintest stars.

The "slit" of ghosts does not align with a fixed wavelength for all spectra as the long slit image of the ghosts will reintroduce the slit curvature that was removed by curving the slit. Hence, it is difficult to place the ghost at a benign spectral position. Additionally, there are few benign spectral regions in which a ghost impact on the GA lines is acceptable.

A data simulator has been produced for HERMES [7], initially to help test the data reduction software. We modified the data simulator to add the production of these ghosts, allowing us to experiment with removal techniques. Fig 19 below shows one of the images produced by this system. This indicates the level of impact that the raw ghost causes on the signal.

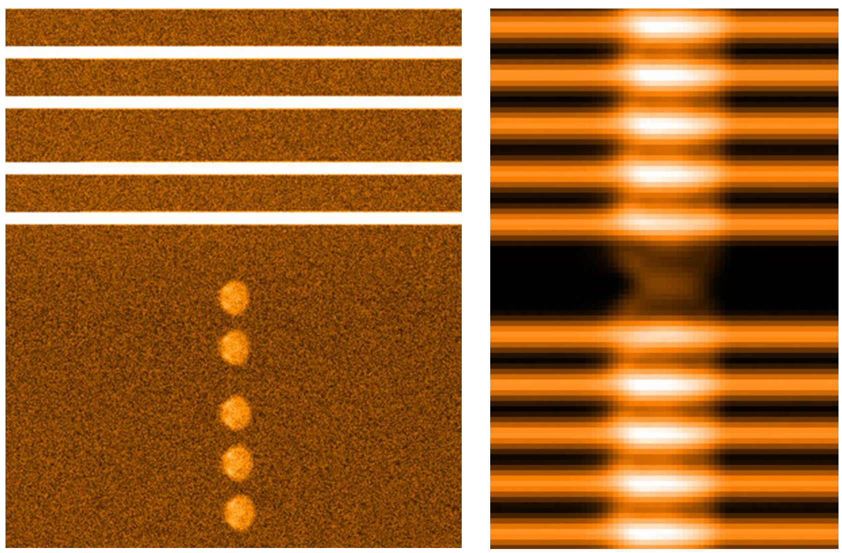

Fig 19. Simulated images of the littrow ghost. In the left figure, input continuum spectra are seen in the top portion, ghost images are seen in the lower half of the image, where the fibres have, in effect, been masked out – to make the ghost clear. The image on the right shows the ghost superimposed on the input continuum, but with the intensity of the ghost increased by a factor of thirty in order to make the shape of the ghost clear. The gap is the gap between two slit blocks.

After investigating approaches using the data simulator, we believe the combination of three techniques will combine to reduce the impact of the ghost: a) The fibre allocation software will incorporate knowledge of the ghost such that it can attempt to place the ghost of a bright object on a similarly bright object rather than on a faint object; b) A simple technique of extracting ghost images from masked fibre flats, scaling them to the actual object intensity and then subtracting the scaled ghost from the image; c) use of optimal fibre extraction techniques [8].

8. Efficiency model

Efficiency models have been developed (Figs 20 and 21) with estimates of the efficiency for all aspects of the instrument. A representative curve is presented here for the HERMES blue channel. The detector spectral coverage is indicated by the straight line at the 0.1 level. The heavy line shows the total system efficiency excluding geometric seeing losses on the fibre ends. The grating efficiency is assumed to be optimized for unpolarized light. A minimum efficiency of 10% is required to achieve a S/N per resolution element of 100 in 1 hour at 14th magnitude for that wavelength bin as required for the GA survey.

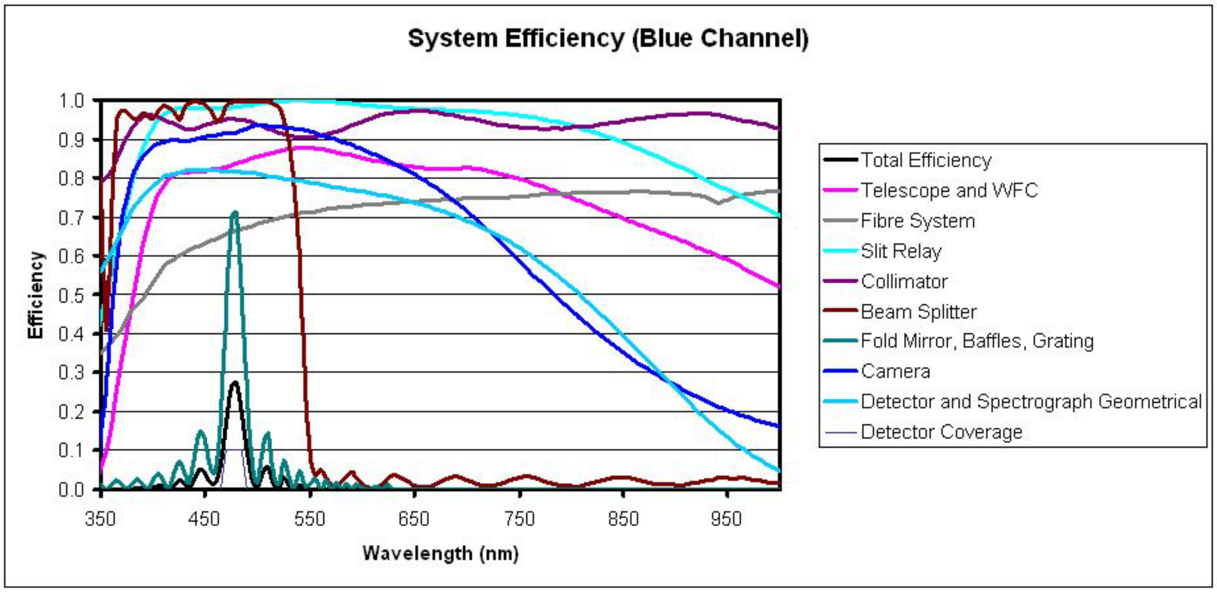

Figure 20. System efficiency for the Blue channel.

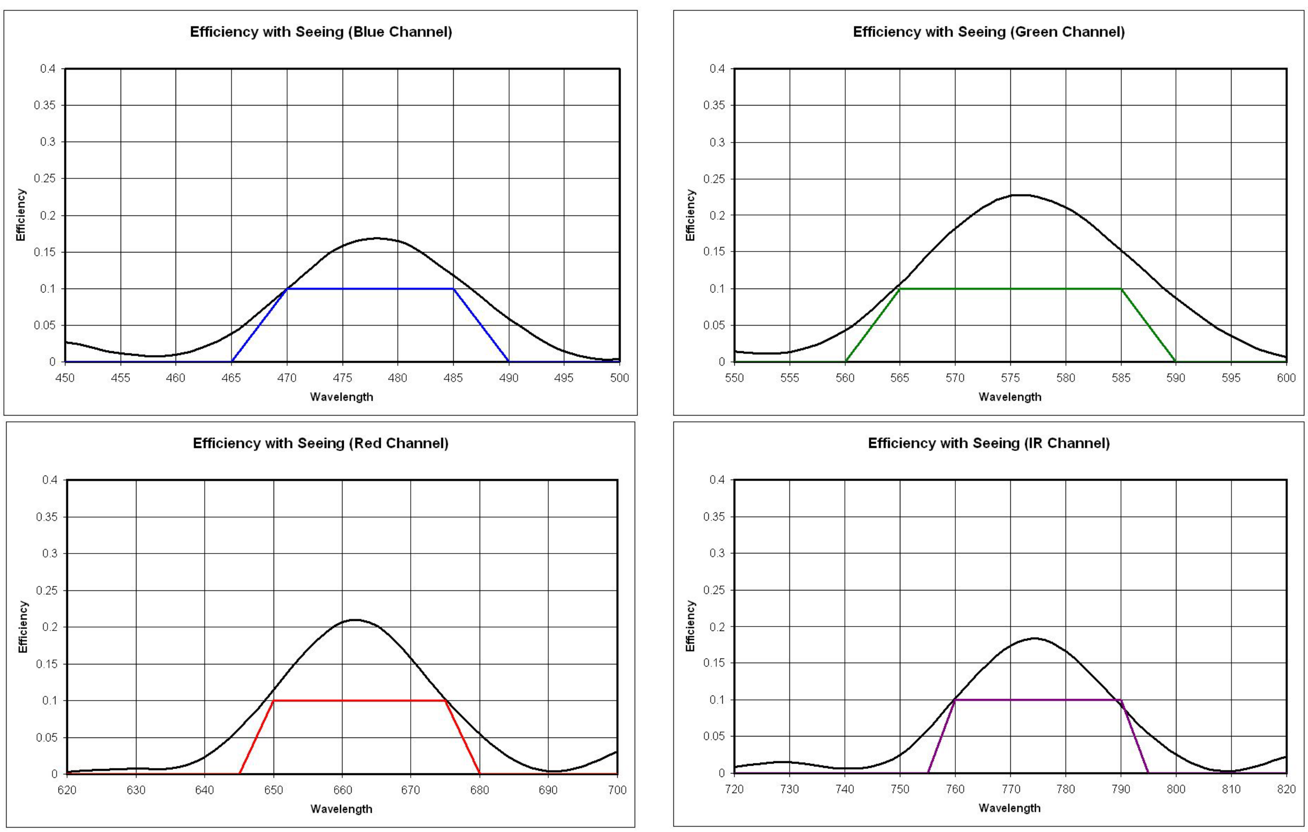

Figure 21. Final predicted efficiency for all channels with median seeing losses included. The flat coloured line indicates the detector coverage and minimum efficiency requirement.

9. Control system

HERMES must integrate into the existing 2dF observation control system [9]. To allow this, a DRAMA[10] software task, implementing a standard control interface, must be provided. This task will provide the standard control interface and instrument status required by the 2dF system and will control the HERMES spectrographs. The 2dF control system GUI will be modified to support four CCD systems rather then the two found in the existing AAOmega/2dF configuration. Additional features such as automated spectrograph focusing and scripted observing will be incorporated to increase observing efficiency.

The control system must interface to various actuators and sensors on the instrument, including servo motor systems, relays and solenoids, switches and analogue sensors. The control system electronics will use COTS (Commercial Off The Shelf) components wherever possible. The Controller Area Network (CAN) distributed industrial fieldbus has been chosen as the control architecture. CAN provides considerable flexibility and a choice of suppliers with a design that minimizes cabling. The CANopen protocol will be used, allowing control from an industrial PC running Linux and providing a good match to the DRAMA environment

To allow early progress on the spectrograph DRAMA control task, a low-level software simulator has been implemented. This implements the CANopen protocol and simulates, at a low level, the devices found in the Spectrograph [10]. The Simulator implementation will be checked against a single axis prototype of the hardware early in the project. This will allow the DRAMA task and 2dF modifications to be developed largely independently of the hardware implementation, providing a reasonable expectation that little effort will be needed to complete it when the hardware is delivered.

10. Calibration

HERMES will use the existing 2dF calibration lamp system, but a couple of issues were identified in the system requirements analysis. At the GA Blue channel, a traditional Quartz Tungsten lamp provides little flux. As a result, a continuum calibration frame in the blue would need an exposure time up to 6 times longer then in the red, which would be operationally difficult. A number of options were examined, including Xenon Short-Arc lamps (lots of bright Xenon lines), LED sources (not bright enough, not enough blue flux) etc. The actual solution proved simple – lamps used in a UV Glue setting system were found to be Quartz Tungsten with a shorter filament – producing more light in the blue. When examined using an Echelle Spectrograph at the HERMES resolution, the response curve was sufficient to allow a single exposure to be used for continuum calibration frames.

The second issue identified was with the Thorium Argon lamps traditionally used for wavelength calibration. The Thorium component produces a rich set of lines for calibration, but in the HERMES GA Infrared channel, two bright Argon lines appear. At any exposure time appropriate for the Thorium lines, these argon lines would saturate the detector, with changes in the detector response possible in subsequent exposures. Experiments were carried out using Thorium lamps with different fill gases and it was found that a Thorium Xenon lamp is a better alternative. It fits the HERMES GA case well and is probably a better lamp in many other cases.

11. Data reduction and abundance analysis

The HERMES GA frames will be processed with two pipelines – a data reduction software to removal of the instrument signature to produce calibrated spectra, and an automated abundance analysis software to determine multi-element abundances. The first part of this will be achieved by adapting the existing AAO Fibre instrument reduction package – 2dFdr[11]. Since adding AAOmega support, significant effort has been put into 2dFdr to ensure its long-term maintainability (removal of dependency on Starlink software, support of up to date compilers and porting to 64 Bit machines, structural changes for improved maintainability). We are now embarking on a series of more then 20 well-defined changes to enable it to achive the best results with HERMES. These include completing the implementation of optimal extraction techniques[11], fine tuning of many processes and investigation of use of multiple CPU's and/or GPUs to increase performance. The resulting output will be fully reduced, sky-subtracted and wavelength calibrated individual stellar spectra.

The abundance analysis software will be developed by the GA Survey team, in close collaboration with the 2dFdr team. The input for the abundance analysis software will be individual spectra, resulting from the above mentioned reduction process. The sequence of the analysis can be summarized as follows: 1. the determination of the stellar atmospheric parameters, initially using photometric estimates and finally the via a chi-squared minimization over a grid of synthetic spectra; 2. the determination of the stellar metallicity via spectra synthesis of Fe and Ti lines; 3. the determination of other elemental abundances via spectra synthesis of the individual lines. A set of unblended lines and a consistent set of atomic data will be pre-selected to gain maximum abundances from minimum spectral coverage. The processing time is estimated to be of the order of several minutes per stars.

4. TIMELINE FOR IMPLEMENTATION

HERMES underwent conceptual design review in mid-2008 and recently passed a preliminary design review. Procurement of long-lead items (optics, detectors, etc.) is underway. Final design of the mechanical components is ongoing and will be reviewed in late 2010. Delivery of the instrument for science is expected to occur in late 2012 or early 2013.

REFERENCES

[1] Barden et al., "Concepts for a high-resolution multi-object spectrograph for galactic archeology on the Anglo-Australian Telescope", SPIE, 7014, 70144J-70144J-12 (2008).

[2] Bland-Hawthorn, J. and Freeman, K. C., "Galactic history: formation & evolution", Memorie della Societa Astronomica Italiana, 77, 1095-1102 (2006).

[3] Bland-Hawthorn, J. and Freeman, K. C., "Galaxy Genesis – Unravelling the Epoch of Dissipation in the Early Disk", Pub. Astron. Soc. Australia, 21(2), 110-120 (2004).

[4] Freeman, K. and Bland-Hawthorn, J., "The New Galaxy: Signatures of Its Formation", Ann. Rev. Astron. and Astrophys., 40, 487-537 (2002).

[5] Bershady M., Westfall, K., Nordsieck, K., Burgh E., "Recombination Ghosts in Littrow Configuration: Implications for Spectrographs Using Volume Phase Holographic Gratings", PASP, 119, 1069–1082 (2007).

[6] Saunders et al. , "AAOmega: a scientific and optical overview", SPIE, 5492, 389 (2004).

[7] Goodwin, M., Smedley, S., Barnes, S., Farrell, T., Barden, S., "Data simulator for the HERMES instrument", SPIE, 7735 (2010).

[8] Sharp, R., Birchall, M., "Optimal Extraction of Fibre Optic Spectroscopy", PASA, 27, 91-103 (2009).

[9] Lewis et. al., "The Anglo-Australian Observatory's 2dF Facility", Mon. Not. R. Astron Soc., 333, 279-299 (2002).

[10] Shortridge, K., Vuong. M., "Faking it for pleasure and profit: the use of hardware simulation at the AAO", SPIE, 7740 (2010) .

[11] Sharp et. al., "Performance of AAOmega: the AAT multi-purpose fiber-fed spectrograph", SPIE, 6269, 62690G (2006).